Strong anharmonic phonon scattering induced giant reduction of thermal conductivity in PbTe nanotwin boundary

Yanguang Zhou,[1,*] Jia-Yue Yang,[2] Long Cheng,[2] and Ming Hu[1,2,†]

[1]*Aachen Institute for Advanced Study in Computational Engineering Science (AICES), RWTH Aachen University, 52062 Aachen, Germany*

[2]*Institute of Mineral Engineering, Division of Materials Science and Engineering, Faculty of Georesources and Materials Engineering, RWTH Aachen University, 52064 Aachen, Germany*

(Received 25 August 2017; revised manuscript received 3 December 2017; published 9 February 2018)

Lead telluride (PbTe) is a renowned thermoelectric material with high energy conversion efficiency in medium to high temperature range. However, the performance of PbTe at room temperature is poor due to its relatively high lattice thermal conductivity, which is difficult to be engineered due to its intrinsic very short phonon mean-free path. By performing systematic first-principles and molecular-dynamics simulations, we report that the room-temperature lattice thermal conductivity of PbTe can be reduced by almost one order of magnitude (86%) using the recent experimentally observed nanotwin structure. The mechanism responsible for the dramatic decrease of thermal conductivity strongly depends on the type and mass of atoms at the twin boundary. For PbTe nanotwinned structures with Te at the twin boundary, phonon transport is dominated by the phonon confinement effect and phonon-twin boundary scattering, and the thermal conductivity converges to the bulk value when half of the periodic length is larger than the dominant phonon mean-free path. The same phenomenon is found in another comparison system of KCl nanotwinned structures. However, when Pb is present at the twin boundary, a scattering mechanism occurs: anharmonicity induced by the twin boundary. Due to the mass difference between Pb and Te, the thermal resistance for Pb residing at the twin boundary is found to be one order of magnitude larger than the case with Te at the twin boundary, which results in much stronger phonon-twin boundary scattering. Consequently, the lowest thermal conductivity of such PbTe nanotwinned structure is only 0.4 W/mK, which is reduced by about sevenfold compared to the bulk value of 2.85 W/mK; finally, the converged thermal conductivity cannot restore the bulk value even when half of the periodic length is much larger than the dominant mean-free path. These results offer useful guidance for the development of PbTe-based thermoelectrics and also suggest that nanotwins are excellent building blocks for enhancing the performance of existing thermoelectrics.

DOI: 10.1103/PhysRevB.97.085304

I. INTRODUCTION

Nanostructuring is a necessary step toward enhancing the energy conversion performance of thermoelectric devices by reducing the lattice thermal conductivity [1–4], since the thermoelectric performance can be characterized by the figure of merit, $ZT = S^2\sigma T/(\kappa_{el} + \kappa_{ph})$, where T, S, σ, κ_{el}, and κ_{ph} are temperature, Seebeck coefficient, electrical conductivity, and the electronic and phononic (lattice) component of thermal conductivity, respectively. However, for the rock-salt thermoelectric materials, such as lead telluride (PbTe) and lead sulfide (PbS), the common nanostructuring method fails to decrease the lattice thermal conductivity, since the intrinsic phonon mean-free path (MFP) in such materials is quite short [5,6] and is typically smaller than the characteristic size that most of nanostructuring can reach. Recent efforts to boost the thermoelectric performance of PbTe have been focused on band structuring via adjusting the doping density, where the aim is to enhance the power factor ($S^2\sigma$) and thus enhance ZT, and indeed ZT around 2 has been achieved [7–9]. Most recently, both experiments [10] and theory [11,12] show that the lower limit of heat transport in the polycrystalline nanostructures can be much below the amorphous limit, which is generally thought to be the lowest possible thermal conductivity in bulk structures. This shows great potential to increase the thermoelectric performance of PbTe by further decreasing the lattice thermal conductivity. At the same time, theoretically speaking, it is also possible to maintain the electronic component via nanostructuring. Therefore, questing for an appropriate nanostructure to achieve the above target may bring revolutionary development for the PbTe-based thermoelectric materials.

In this paper, we employ first-principles and molecular-dynamics simulations to show that by introducing recently fabricated rock-salt nanotwinned structures [13,14] into PbTe and KCl (KCl is chosen as a comparative partner here since nanotwins can be easily generated in KCl experimentally [15]), the lattice thermal conductivity can be reduced by almost one order of magnitude. Although there is no direct experimental report of PbTe nanotwinned structures so far, there are many similar structures, such as PbS nanotwin, MnS nanotwin, and KCl nanotwin that have already been fabricated in experiments as we mentioned above. Considering that S belongs to the same group as Te, we speculate that our theoretical models of PbTe nanotwinned structures will stimulate experimentalists to synthesize similar structures as

*yanguang.zhou@rwth-aachen.de
†hum@ghi.rwth-aachen.de

PbS. Such significant low thermal conductivity is induced by the bi- or trimodal phonon scattering at the twin boundary. Different phonon scattering mechanisms are identified with periodic length of the twin boundary increasing: from the combined effect of phonon confinement, which comes from the distortion of phonon dispersion when the size scale goes down to nanoscale, phonon boundary scattering and boundary anharmonicity, to phonon boundary scattering and boundary anharmonicity, and then to pure boundary anharmonicity. Both the lowest and the bulklike thermal conductivity (half of the periodic length is comparable to the dominant MFP in its bulk counterpart) of PbTe nanotwinned structures depend strongly on the type and mass of atoms at the twin boundary. It is also worth noting that the electronic structure and the transport properties might change in the nanotwinned structures, which could be intuitively confused with conventional grain boundaries. Here, the authors just assume the electrical transport properties will stay unchanged. Actually, the nanotwin could even have a positive effect on electrical transport properties, or in other words, the power factor can be even enhanced by the nanotwinned structures. In our recent paper [16], the power factor has been proven to be improved by around 2 times in Si-based nanotwinned structures [16]. In this work, we mainly focus on the mechanisms leading to reduction of lattice thermal conductivity in PbTe nanotwin.

II. STRUCTURE AND COMPUTATIONAL METHODOLOGY

The atomic-resolution microscopy [13–15] and theory demonstrate that both cations (K or Pb) and anions (Cl or Te) can stay at the twin boundary (Fig. 1). Comparing to its bulk counterpart [Fig. 1(b)], it is easy to find that the underlying Bravais lattice in the twinned structure remains intact [Fig. 1(c) and Supplemental Material, Fig. S7 in Ref. [17–26]). By rotating the bulk structure along the [111] axis by 180° and then putting the rotated and original ones together, the nanotwinned structure is obtained. Since electronic transport is not sensitive to atomic mass, one expects that the electrical conductivity is not affected by the twin boundaries, whereas the mass disparity across the twin boundary would have significant effect on the thermal transport [27,28] (see results below for details). We have to emphasize that it is impossible to fabricate *perfect* nanotwinned bulk structure experimentally. However, since the phonon MFP in PbTe is quite small (the maximum MFP in bulk crystalline PbTe is around 10 nm, as shown in Fig. S3 [17]), it is suitable to use a perfect PbTe model structure to represent the polycrystalline heterostructure with grain size large than 10 nm [Fig. S3 [17]), which is realizable in experiments. In this case, the phonon boundary scattering can be ignored and therefore the lattice thermal conductivity will not be affected by the grain boundaries. Introducing nanotwin into the grains, the phonon MFP will become smaller since the phonons can be scattered further by the twin boundary, and thus it is appropriate to ignore the effect of grain boundaries when the grain size is larger than 10 nm. In addition, it is quite easy to fabricate the polycrystalline nanotwinned heterostructures with large grain size (e.g., larger than 10 nm) [29–32]. Moreover, the nanotwinned structure has been proven to have positive effect on electrical transport properties both experimentally [29,33] and theoretically [16,34]. At the same time, the nanotwinned structure with periodic length as small as 1.5 nm has been fabricated in experiments successfully [31]. What is more, the PbS (quite similar to PbTe) nanotwin polycrystalline heterostructure has been fabricated successfully [35,36]. In this work, the lattice thermal conductivity is computed using the Green-Kubo (GK) formula [19] through equilibrium molecular-dynamics simulation (EMD) (see Refs. [11,37] for computational details). Atomic interactions are depicted by the Buckingham potential for PbTe [20] and Born-Huggins-Mayer potential for KCl [38] with long-range Coulombic force considered in the reciprocal space (energy convergence criteria of 1×10^{-4} eV). For each case, 30 independent runs are performed in order to obtain a stable average thermal conductivity (κ). The autocorrelation time for GK-EMD is chosen as 50 ps, which is long enough to obtain the steady thermal conductivity due to the inherent small average phonon relaxation time of PbTe and KCl (see Sec. I in Ref. [17] for details). All the classical MD simulations are performed with the LAMMPS package [39]. We first run 50 ps with a time step of 1 fs to reach the target temperature using the *NVT* (constant particles, volume, and temperature) ensemble. Then, for the equilibrium molecular-dynamics simulations, we run 2 ns with the *NVE* (constant particles, volume, and energy) ensemble to generate the instant heat currents that are used to calculate the thermal conductivity via Green-Kubo theory [19]. The size effect in GK-EMD simulation is also tested (Sec. II in Ref. [17]). For nonequilibrium molecular dynamics (NEMD) simulations, fixed boundary conditions are applied to both ends of the system. Near to the fixed boundaries, a hot and cold reservoir with respective temperature of 325 and 275 K is applied such that a temperature gradient is established along the concerned direction (z direction in our simulations) after running 3 ns. In the last 1-ns NEMD run, we output the trajectories of atomic velocities every five time steps for the transmission coefficient calculation [Eq. (1) below]. The room-temperature thermal conductivity of bulk PbTe and KCl computed using the classical potential is 2.85 and 5.1 W/mK, respectively. In comparison, the experimental value for bulk PbTe and KCl is 2.4 W/mK [7] and 6.5 W/mK [40], respectively. The difference between theoretical and experimental results (15.7% for PbTe and 21.5% for KCl) is acceptable considering many factors involved, such as classical potential used in our

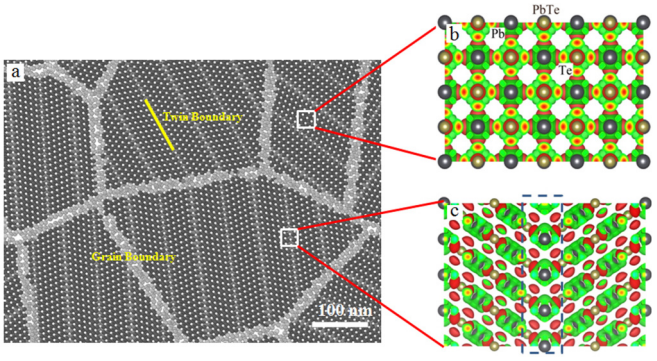

FIG. 1. (a) Polycrystalline nanotwin PbTe structure. Charge density difference of (b) bulk PbTe, (c) PbTe nanotwinned structure with Pb at twin boundary.

GK-EMD simulation, errors in experimental measurement, the quality of the samples in experiments, etc. Moreover, all our results reported here are calculated using the same methods and the same interatomic potential, and therefore this difference is believed to have no impact on our comparison and conclusion. Another important disadvantage existing in the classical MD simulation, the Boltzmann distribution of atom trajectory, should also have no effect on our results, since the Debye temperature of PbTe and KCl is only 136 and 235 K, respectively (the Boltzmann distribution approximates to Bose-Einstein distribution at room temperature).

All the first-principles calculations are computed using the Vienna Ab initio Simulation Package (VASP) based on the density-functional theory. Periodic boundary conditions are applied in all three directions. The pseudopotential with generalized gradient approximation, parametrized by Perdew-Burke-Ernzerhof [41], is used for the exchange-correlation functional. A plane basis with cutoff energy of 310 eV for PbTe and 341 eV for KCl and the Monkhorst-Pack scheme [42] is used to generate an $8 \times 8 \times 8$ (bulk) and $4 \times 8 \times 8$ (nanotwinned structures) k-point mesh. Before any electrostatic potential or interatomic force constant calculation, the atomic structures and cell size are fully relaxed until the energy difference and the Hellman-Feynman force are converged within 1×10^{-4} eV and 5×10^{-3} eV/Å, respectively. Spin-orbit interaction is included. Then, we run Born-Oppenheimer molecular dynamics for 30 ps to obtain the atomic velocity for the time-domain normal-mode analysis (TDNMA) calculations [24], in which a time step of 3 fs is chosen for both KCl and PbTe and the k-point mesh is shifted to $4 \times 8 \times 8$. In our paper, we only use first-principle-based TDNMA to calculate the lattice thermal conductivity of PbTe and KCl nanotwinned structures with the shortest periodic length of 2.3 nm due to the computational cost (Fig. 2).

III. RESULTS AND DISCUSSION

A. Extremely low thermal conductivity induced by twin boundary

We now examine the effect of twin boundary on the thermal conductivity (Fig. 2). For KCl nanotwinned structures, whenever the anions or cations are present at the twin boundary, the lattice thermal conductivity is as low as around 0.7 W/mK, which is only 13% of its bulk value. For nanotwinned PbTe with Te at the twin boundary, the thermal conductivity can be reduced by around 3.5-fold compared to its bulk value and reach a quite low value of only 0.8 W/mK. When the cations (Pb) are at the twin boundary, the lowest lattice thermal conductivity can be lowered to only 0.4 W/mK, which is reduced by around sevenfold from the bulk value. The periodic length of nanotwin for these smallest values in our simulations is around 2 nm, which has already been realized in experiments [31]. To confirm the accuracy of our results, first-principles equilibrium molecular-dynamics simulation coupled with TDNMA is implemented to get the lattice thermal conductivity of PbTe and KCl nanotwinned structures with the shortest periodic length of 2.3 nm. The results are shown in Fig. 3 and the calculation details can be found Sec. III in Ref. [17]. The good agreement between our classical GK-EMD simulation

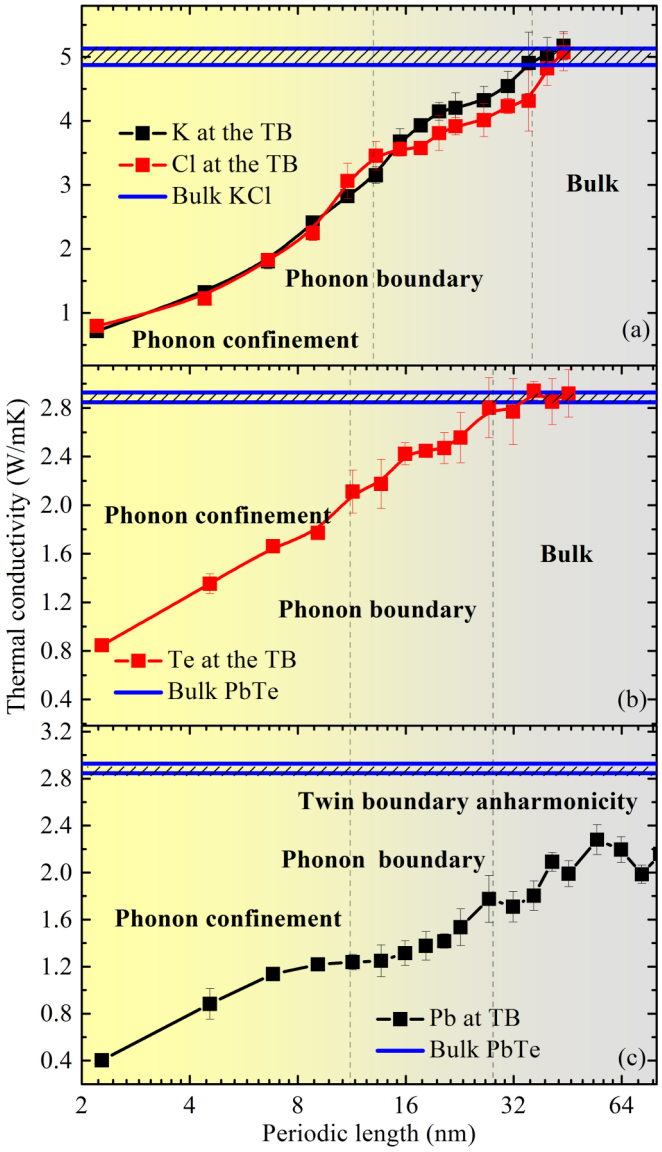

FIG. 2. Periodic length-dependent thermal conductivity of nanotwinned structures calculated by Green-Kubo equilibrium molecular-dynamics simulation for: (a) KCl, (b) PbTe with Te at twin boundary, and (c) PbTe with Pb at TB. The blue solid lines denote the thermal conductivity of bulk KCl and PbTe. Different shading color represents different regimes of phonon scattering.

[the columns with pattern in the right panel of Fig. 3(a)] and first-principles calculation enables us to believe that classical MD simulations are good enough to capture the thermal transport properties of PbTe and KCl (Fig. 3). The significantly low thermal conductivity is caused by phonon confinement effect and phonon boundary scattering in KCl, whereas in PbTe, when Pb is at the twin boundary, an additional mechanism, namely boundary anharmonicity, which causes the huge difference in the scattering rate (inverse of relaxation time) in the PbTe nanotwinned structures [Fig. 3(b)], is also responsible for the extremely low thermal conductivity (detailed discussion can be found below). Here, our smallest lattice thermal conductivity (around 0.4 W/mK) is more or less equal to the minimal value of the quantum-dot PbTe superlattice reported in Ref. [41],

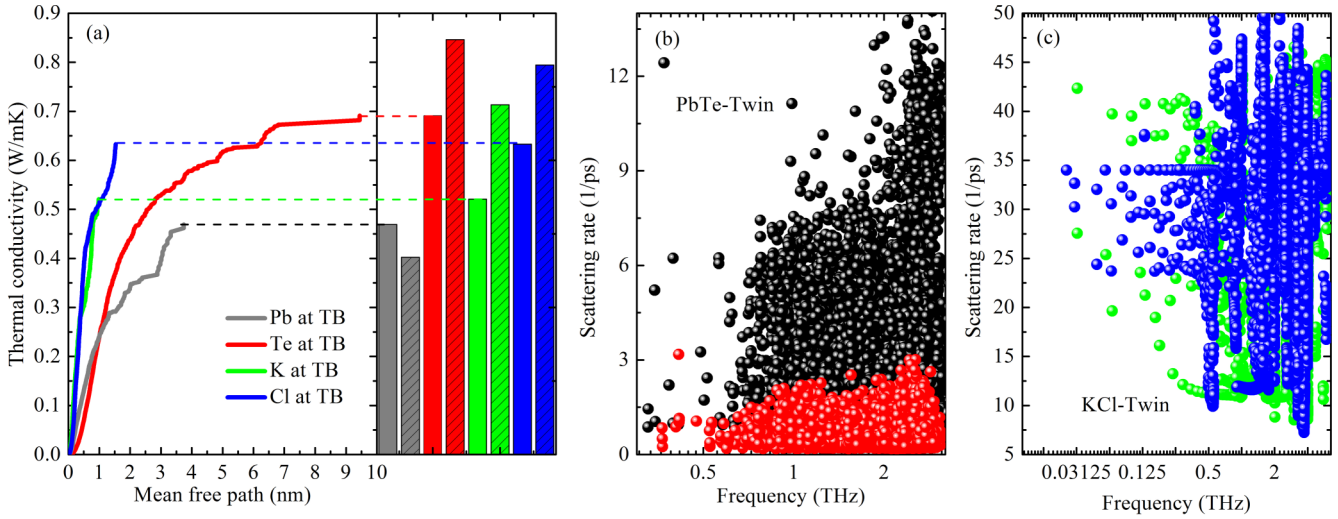

FIG. 3. (a) Comparison of thermal conductivity of PbTe and KCl nanotwinned structures calculated by first-principles equilibrium molecular dynamics coupled with TDNMA (without shaded pattern) and classical GK-EMD (with shaded pattern). (b) Scattering rate for PbTe nanotwinned structures (black and red circles are results for Pb and Te at the twin boundary, respectively). (c) Scattering rate for KCl nanotwinned structures (blue and green circles are results for Cl and K at the twin boundary, respectively). The periodic length for all cases is 2.3 nm. Only the columns with shaded pattern are calculated by classical MD [right panel in (a)]. All other results here are computed by first-principles equilibrium molecular-dynamics simulation coupled with TDNMA.

since the 0.05 W/mK error bar can be easily generated from the experiments. However, it is quite difficult to fabricate such quantum-dot superlattice structure in experiments, which will restrict its large-scale application. The most important point is that the nanotwinned structure has been proven to have the ability to improve the electrical transport properties (power factor) both experimentally [29,33] and theoretically [16], which is amazing for thermoelectrics. Furthermore, it has been experimentally proven that the nanotwin can improve the mechanical performance of materials such as strength and plasticity [24,30,42], which is quite good for improving the stability of thermoelectric devices as well. With the periodic length of the twin boundary increasing, it is not surprising to find the lattice thermal conductivity increasing, since the phonon boundary scattering and phonon confinement effect become weaker or even disappear. When the periodic length is increased to the dominant mean-free path of phonons (∼30 nm for KCl and ∼10 nm for PbTe, detailed results shown in Sec. IV in Ref. [17]), the lattice thermal conductivity converges to the bulk value for KCl nanotwinned structures regardless of the type of the ions at the twin boundary and PbTe nanotwinned structure with Te at the twin boundary [Figs. 2(a) and 2(b)]. This indicates that when the periodic length is long enough, only inherent bulk phonon-phonon scattering exists in the nanotwinned structures and thus the effect of both phonon-twin boundary and phonon confinement can be ignored. However, when Pb is at the twin boundary, it is intriguing to observe that the lattice thermal conductivity (only around 2.2 W/mK) of the PbTe nanotwinned structure with long enough periodic length (much longer than the dominant MFP) is still considerably smaller than the bulk value (2.85 W/mK), which means the phonon boundary scattering and phonon confinement are not enough anymore [Fig. 2(c)]. Even when half of the SL periodic length is much larger than the dominant MFP, the thermal conductivity of the PbTe nanotwin with Pb at the twin boundary is much lower than the bulk value. Changing the mass between Pb and Te will not change our conclusions (Sec. VII in Ref. [17]), which means the large mass difference is not the main reason for the observed phenomenon. In the following, we will explain the underlying mechanism for the giant reduction of lattice thermal conductivity and the much lower bulklike thermal conductivity for the PbTe nanotwinned structure with Pb at the twin boundary.

B. Large thermal resistance at the twin boundary induced by phonon-twin boundary scattering

From the structural point of view, the only difference between nanotwinned structure and bulk crystalline is the atom arrangement at the twin boundary. Therefore, it is intuitive to reveal the underlying mechanism by starting with phonon scattering at the twin boundary using NEMD simulation. Firstly, we show the temperature distribution in the nanotwinned structures in Fig. 4. It is interesting to find that, for KCl nanotwinned structures, the temperature drop at the twin boundary is almost the same whenever cations or anions are present at the twin boundary [Figs. 4(a) and 4(b)], which is consistent with the similar values of lattice thermal conductivity of KCl nanotwinned structures [Fig. 2(a)]. However, for PbTe nanotwinned structures, the temperature drop at the twin boundary strongly depends on the type of the atoms stacking on the twin boundary. For the PbTe nanotwinned structure with cation (Pb) at the twin boundary, the temperature drop is one order of magnitude larger compared to the structure with anions (Te) at the twin boundary [Figs. 4(c) and 4(e)]. As a result, the interfacial thermal resistance for the case of cation (Pb) at the twin boundary is much larger than that with anion (Te) at the twin boundary. One reason for such a huge difference is the large mass disparity at the twin boundary [28]. Generally speaking, it is more difficult for phonons to transport from Te to

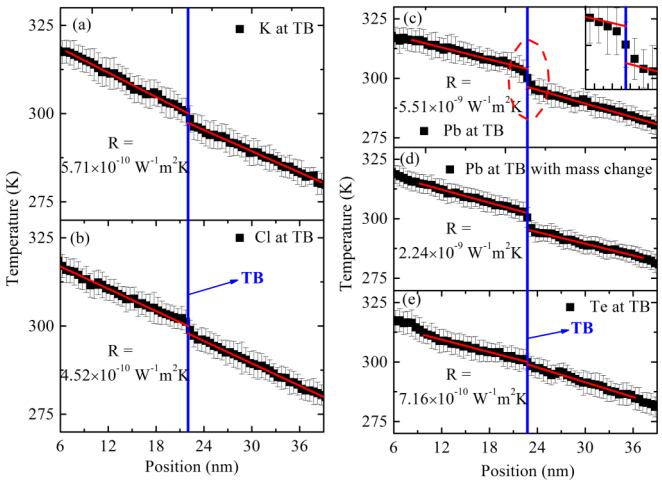

FIG. 4. Temperature distribution and thermal boundary resistance for (a) KCl nanotwinned structure with K at the TB, (b) KCl nanotwinned structure with Cl at the twin boundary, (c) PbTe nanotwinned structure with Pb at the twin boundary, (d) PbTe nanotwinned structure with Pb at the twin boundary and the mass of Pb and Te is exchanged, (e) PbTe nanotwinned structure with Te at the twin boundary. The blue vertical line stands for the position of the twin boundary and the dashed red circle implies the temperature jump at the twin boundary due to the anharmonicity. (Inset) Detailed real temperature distribution across the PbTe twin boundary with red lines denoting the linear temperature distribution. The periodic length for all cases is 41 nm.

Pb than the reverse direction. This is because the same phonon should have larger group velocity in the lighter mass system (Te in our case) [28], which has a larger frequency range. This means a part of the phonons with frequency larger than the heavy atom's cutoff frequency are strongly suppressed from the Te side (detailed discussions can be also found below). To prove our viewpoint, we switch the atom mass of Pb and Te [Fig. 4(d)] and keep the rest of the computational conditions unchanged. It is expected to find that the interfacial thermal resistance decreases but is still much larger than that of the PbTe nanotwinned structure with anion (Te) at the twin boundary [Fig. 4(e)]. This means both the difference in the atom mass and the interatomic interaction should be responsible for the huge difference of interfacial thermal resistance as shown in Figs. 4(c) and 4(e).

In order to understand the frequency level phonon scattering at twin boundaries, the thermal transmission coefficient is calculated via [23,28,43,44]

$$\Gamma(\omega) = -\frac{2i}{\omega k_B \Delta T} \sum_{i\in L,\ j\in R} \sum_{\alpha\beta} \left[\Phi_{ij}^{\alpha\beta} \langle \tilde{v}_j^{\beta}(\omega) \tilde{v}_i^{\alpha *}(\omega) \rangle\right], \quad (1)$$

where the bracket represents the time average, α and β stand for the direction (x, y, or z), v_i and v_j are the velocities of atom i and j, respectively, Φ_{ij} is the second-order force constants, k_B and ΔT are the Boltzmann constant and temperature drop, respectively. Figure 5(a) shows that, for the PbTe nanotwinned structure with Pb at the twin boundary, the low-frequency phonons (0–2 THz) are strongly scattered compared to the nanotwinned structure with Te at the twin boundary, which leads to a huge difference in the interfacial thermal resistance as

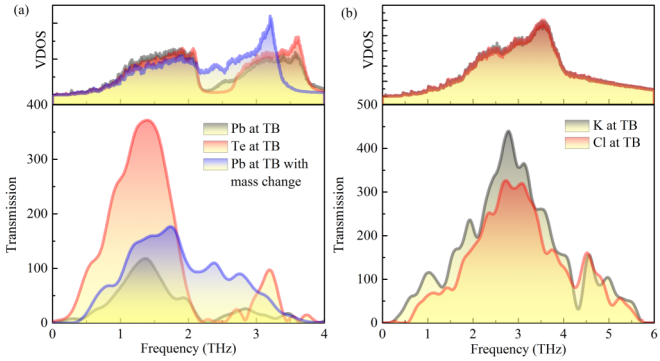

FIG. 5. Phonon vibrational density of states and transmission coefficient at the twin boundary for (a) PbTe nanotwinned structures and (b) KCl nanotwinned structures. The periodic length for all cases is 41 nm.

we found in Figs. 4(c) and 4(e). By switching the mass between Pb and Te atoms, the high-frequency phonons (2–3.5 THz) can pass through the twin boundary, since more phonon states appear in this region [Fig. 5(a)]. However, the low-frequency phonons (0–2 THz) are still strongly scattered by the twin boundary, which proves again that the mass difference between Pb and Te at the twin boundary is not the only factor for the above huge difference in the interfacial thermal resistance. For KCl nanotwinned structures, the phonon transmission at the two different twin boundaries is almost the same [Fig. 5(b)], which indicates the type of atom at the twin boundary has a minor effect on the trend of lattice thermal conductivity as shown in Fig. 2(a).

C. Underlying mechanism of the significantly low thermal conductivity

Meanwhile, in the diffusive thermal transport regime, the thermal conductivity of nanotwinned structures (κ_{nanotwin}) can be calculated as [45]

$$\frac{1}{\kappa_{\text{nanotwin}}} = \frac{1}{\kappa_0} + \frac{R}{d_{\text{eff}}}, \quad (2)$$

in which [24,46]

$$d_{\text{eff}} = \frac{1+P}{1-P} d, \quad (3)$$

where κ_0 is the bulk lattice thermal conductivity, R is the thermal resistance at the twin boundary, d_{eff} is the effective width between two neighboring twin boundaries, d is the half of the periodic length of twin boundaries, and P is the specularity parameter which can describe the strength of phonon boundary scattering [47,48]. Equation (3) has been widely used to discuss the effect of interface structures and geometry on thermal transport [24,46]. Clearly, $P = 1$ corresponds to the ideal smooth twin boundary without phonon boundary scattering. In other words, the effective length between two twin boundaries is infinite, which means the phonons will never be scattered by the twin boundary, since they can never travel so long from one twin boundary to the next twin boundary. On the other hand, when the twin boundary is quite rough (such as the situation for the polycrystalline structure [11]) or has a large discontinuity in the vibrational frequency (the

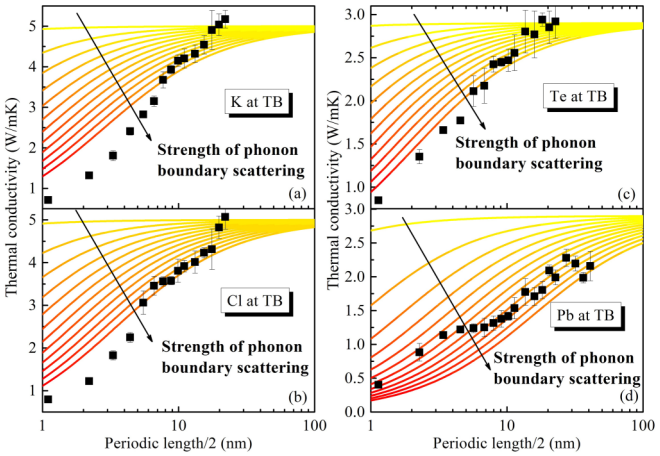

FIG. 6. Thermal conductivity of nanotwinned structures (solid lines) by only considering the phonon boundary scattering: (a) KCl nanotwin with K at the twin boundary, (b) KCl nanotwin with Cl at the twin boundary, (c) PbTe nanotwin with Te at the twin boundary, and (d) PbTe nanotwin with Pb at the twin boundary. The arrow indicates the increase of the strength of phonon boundary scattering. The filled squares are results from GK-EMD simulations.

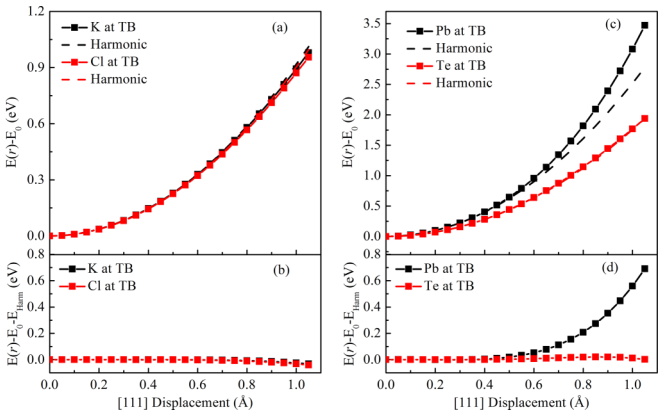

FIG. 7. Potential energy changes for displacement in the [111] direction for (a) KCl and (c) PbTe nanotwinned structure. The corresponding anharmonic energy for (b) KCl and (d) PbTe nanotwinned structure.

situation in our cases), the phonons can be scattered strongly, which means $P = 0$. Here, we would like to point out that the specularity parameter strongly depends on the geometry and structure. We consider such effect via different P parameter in Eq. (3). In our paper, the nanotwin can be also treated as a special superlattice structure, and therefore we believe that it is appropriate to apply Eq. (3) to depict the phonon boundary scattering. Theoretical prediction in Fig. 6 (solid lines) clearly shows that the stronger the phonon boundary scattering, the smaller the lattice thermal conductivity of the nanotwinned structures with the same periodic length, or equivalently, the smaller the d_{eff}. For KCl nanotwinned structures [Figs. 6(a) and 6(b)], it is surprising to find that below a critical periodic length (around 18 nm for KCl nanotwin with K at the twin boundary and about 10 nm for that with Cl at the twin boundary), the MD result is even below the lowest limit of theoretical prediction (the strongest phonon boundary scattering), which indicates that only considering phonon boundary scattering is obviously not enough. It is well known that the phonon dispersion will be depressed for the nanostructures with small boundary width, e. g., grain size, diameter of nanowires, or periodic length of superlattices [49–53], which will lead to the reduction of group velocity and then the lattice thermal conductivity will be reduced. Such effect is usually called phonon confinement effect, which is inevitable in the small size structures. When the phonon confinement effect is strong, the assumption in Eq. (2), namely the phonon dispersion in nanostructures is the same as that in its bulk counterpart, is questionable. In our cases, the nanotwinned structure can be regarded as a special superlattice structure, which means it should also have the phonon confinement effect. From our phonon dispersion results (Sec. V in Ref. [17]), we truly find that the depression of the dispersions mentioned above exists in the nanotwinned structures when the periodic length is small. Above the critical periodic length, the MD results can always map into the results that only consider the phonon-twin boundary scattering. In such cases, the dominant mechanism for the reduction of thermal conductivity is phonon-twin boundary scattering. Finally, when half of the periodic length (∼26 nm) is approaching the dominant MFP (∼30 nm), the thermal conductivity converges to the bulk value. For PbTe nanotwinned structures with Te at the twin boundary [Fig. 6(c)], we find the similar phenomenon discussed above: The critical periodic length for phonon confinement and boundary scattering is ∼6 and 14 nm, respectively. For PbTe nanotwinned structures with Pb at the twin boundary [Fig. 6(d)], it seems that only considering the phonon boundary scattering is enough since all our MD results can be mapped onto the theoretical predictions. However, after long deliberation, it is easy to find two contradictions: (1) the phonon confinement cannot be avoided in the cases with small periodic length, since the phonon dispersion is considerably depressed (Sec. V in Ref. [17]); (2) the largest periodic length of the PbTe nanotwin with Pb at the twin boundary (TB) is around 80 nm; considering the structure and geometry of the TB, we obtain d_{eff} here to be in the range from 36 to 39 nm, which is larger than the dominant MFP (∼10 nm) in PbTe (Sec. IV in Ref. [17]), meaning that the phonons cannot be scattered by the twin boundary. When the periodic length of the PbTe nanotwin is approaching 20 nm, intuitively the thermal conductivity should also saturate to its bulk value [Fig. 2(b)]. However, for the PbTe nanotwin with Pb at the twin boundary, the thermal conductivity is still much lower than its bulk value even when the periodic length of SL is as large as 80 nm (the largest case we can consider due to our computational capacity). Then, the questions are, what is the reason for these two contradictions? How do they affect the thermal conductivity?

Before we answer the above questions, we firstly calculate the anharmonic energy (E_{Anharm}) by

$$E_{\text{Anharm}} = E(r) - E_0 - E_{\text{Harm}}, \tag{4}$$

where $E(r)$, E_0, and E_{Harm} are the energy of the system after the movement of atoms, the original energy of the system, and the harmonic fitting energy of the potential well, respectively. As shown in Figs. 7(a) and 7(b), the anharmonic contribution induced by the cations or anions at the twin boundary can be ignored in KCl nanotwinned structures. In contrast, for PbTe

nanotwinned structures [Figs. 7(c) and 7(d)], it is astonishing to find that giant anharmonicity is present when the Pb atoms are at the twin boundary, while Te atoms at the twin boundary have no noticeable anharmonicity. Changing the distance between two twin boundaries (half of the periodic length) or the atom mass at the twin boundary will not change our conclusion (Sec. VI in Ref. [17]). It is well known that the Pb in PbTe is quite special since it can drive long-range interaction by resonant bonding [6]. The extremely strong anharmonicity in PbTe is also caused by such long-range interactions. In the classical potential, such a long-range interaction is considered via the Coulombic force. For the PbTe nanotwin with Pb at the twin boundary, it can be regarded as the bulk PbTe with an additional Pb layer. Therefore, there is no surprise to find that the anharmonicity in the PbTe nanotwin with Pb at the twin boundary is even stronger than that in bulk PbTe. How these additional Pb layers exactly affect the anharmonicity will be studied in our future calculations. Now, we can explain the above contradictions: in addition to the huge temperature drop at the Pb twin boundary, giant anharmonic effect can be also induced by the twin boundary, which will cause a strong nonlinear effect near the twin boundary [the real temperature distribution actually deviates from the ideal linear line as shown in the inset of Fig. 4(c)], and then enhance the phonon-phonon scattering and decrease the thermal conductivity. It is also worth noting that, since such anharmonic effect is independent on the periodic length and atom mass, the converged thermal conductivity for the PbTe nanotwinned structure with Pb at the twin boundary (with and without mass change) should be lower than the corresponding bulk value as shown in Fig. 2(c) and Sec. VII in Ref. [17]. We also calculate the Grüneisen parameter for the nanotwinned structures with Pb and Te at the twin boundary (the results can be found in Sec. VIII in Ref. [17]). It is clearly shown that the nanotwinned structure with Pb at the twin boundary has a larger Grüneisen parameter comparing to that with Te at the twin boundary, especially for low-frequency acoustic phonons, which are the major heat carrier in nanotwinned PbTe. Now, the reason for the giant reduction of thermal conductivity in the PbTe nanotwinned structures is clear: phonon transport is governed by the combined effect of phonon confinement effect, phonon-twin boundary scattering, and anharmonicity induced by the twin boundary. The first two mechanisms apply to the case of Te at the twin boundary and the third mechanism is the additional effect only valid for the case of Pb at the twin boundary.

IV. CONCLUSIONS

In summary, by performing molecular-dynamics simulation and first-principles calculations, the thermal transport in PbTe and KCl nanotwinned structures is studied. About an order of magnitude reduction (up to 86%) in the thermal conductivity of nanotwinned structures relative to the corresponding bulk value is observed. The thermal conductivity of the nanotwinned structures depends monotonically on the periodic length and converges to their corresponding bulk value except the PbTe nanotwinned structure with Pb at the twin boundary. By calculating the phonon mean-free path and the strength of phonon-twin boundary scattering, two or three combined mechanisms are responsible for the giant reduction of thermal conductivity. For KCl nanotwinned structures with either K or Cl at the twin boundary and PbTe nanotwinned structures with Te at the twin boundary, when the periodic length is smaller than the critical length, both phonon confinement effect and phonon-twin boundary scattering are responsible for the extremely low thermal conductivity, while when the periodic length is beyond this critical value, phonon-twin boundary scattering is dominant in the reduction of thermal conductivity. Finally, the thermal conductivity will converge to the corresponding bulk value when the periodic length is considerably larger than the dominant phonon mean-free path. However, for the PbTe nanotwinned structure with Pb at the twin boundary, the third mechanism, namely anharmonicity induced by the twin boundary, is found to be related to the huge reduction of thermal conductivity. Due to the giant anharmonicity induced by the twin boundary, the obtained thermal conductivity in this kind of twin structure cannot go back to the level of the corresponding bulk crystalline PbTe (23% lower) even when half of the periodic length is significantly larger than the dominant mean-free path. We expect that the present theoretical results will generate tremendous interest for experimentalists to fabricate PbTe nanotwinned structures and bring a revolutionary solution to the PbTe-based thermoelectrics.

ACKNOWLEDGMENTS

Simulations were performed with computing resources granted by the Jülich Aachen Research Alliance-High Performance Computing (JARA-HPC) from RWTH Aachen University under Project No. jara0166.

[1] S. I. Kim, K. H. Lee, H. A. Mun, H. S. Kim, S. W. Hwang, J. W. Roh, D. J. Yang, W. H. Shin, X. S. Li, and Y. H. Lee, Science **348**, 109 (2015).
[2] B. Poudel, Q. Hao, Y. Ma, Y. Lan, A. Minnich, B. Yu, X. Yan, D. Wang, A. Muto, and D. Vashaee, Science **320**, 634 (2008).
[3] A. I. Boukai, Y. Bunimovich, J. Tahir-Kheli, J. Yu, W. A. Goddard III, and J. R. Heath, Nature (London) **451**, 168 (2008).
[4] A. I. Hochbaum, R. Chen, R. D. Delgado, W. Liang, E. C. Garnett, M. Najarian, A. Majumdar, and P. Yang, Nature (London) **451**, 163 (2008).
[5] Z. Tian, J. Garg, K. Esfarjani, T. Shiga, J. Shiomi, and G. Chen, Phys. Rev. B **85**, 184303 (2012).
[6] S. Lee, K. Esfarjani, T. Luo, J. Zhou, Z. Tian, and G. Chen, Nat. Commun. **5**, 3525 (2014).
[7] Y. Pei, X. Shi, A. LaLonde, H. Wang, L. Chen, and G. J. Snyder, Nature (London) **473**, 66 (2011).
[8] A. D. LaLonde, Y. Pei, and G. J. Snyder, Energy Environ. Sci. **4**, 2090 (2011).
[9] Y. Pei, Z. M. Gibbs, A. Gloskovskii, B. Balke, W. G. Zeier, and G. J. Snyder, Adv. Energy Mater. **4**, 1400486 (2014).

[10] J. P. Feser, E. M. Chan, A. Majumdar, R. A. Segalman, and J. J. Urban, Nano Lett. **13**, 2122 (2013).
[11] Y. Zhou and M. Hu, Nano Lett. **16**, 6178 (2016).
[12] C. Melis and L. Colombo, Phys. Rev. Lett. **112**, 065901 (2014).
[13] Y. B. Xue, Y. T. Zhou, D. Chen, and X. L. Ma, J. Alloys Compd. **582**, 181 (2014).
[14] Y. T. Zhou, Y. B. Xue, D. Chen, Y. J. Wang, B. Zhang, and X. L. Ma, Sci. Rep. **4**, 5118 (2014).
[15] H. Hattori, J. Cryst. Growth **66**, 205 (1984).
[16] Y. Zhou, X. Gong, B. Xu, and M. Hu, Nanoscale **9**, 9987 (2017)
[17] See Supplemental Material at http://link.aps.org/supplemental/10.1103/PhysRevB.97.085304, which includes Refs. [18–25], for computational details, phonon mean-free path and dispersion, size effect on results, and how to choose the parameters.
[18] D. Torii, T. Nakano, and T. Ohara, J. Chem. Phys. **128**, 44504 (2008).
[19] R. Kubo, Rep. Prog. Phys. **29**, 255 (1966).
[20] B. Qiu, H. Bao, G. Zhang, Y. Wu, and X. Ruan, Comput. Mater. Sci. **53**, 278 (2012).
[21] G. P. Srivastava, *The Physics of Phonons* (CRC Press, Boca Raton, FL, 1990).
[22] A. Togo and I. Tanaka, Scr. Mater. **108**, 1 (2015).
[23] Y. Zhou and M. Hu, Phys. Rev. B **92**, 195205 (2015).
[24] Y. Zhou, X. Zhang, and M. Hu, Phys. Rev. B **92**, 195204 (2015).
[25] W. Li, J. Carrete, N. A. Katcho, and N. Mingo, Comput. Phys. Commun. **185**, 1747 (2014).
[26] A. Maiti, G. D. Mahan, and S. T. Pantelides, Solid State Commun. **102**, 517 (1997).
[27] Y. Zhou, X. Zhang, and M. Hu, Nanoscale **8**, 1994 (2016).
[28] Y. Zhou and M. Hu, Phys. Rev. B **95**, 115313 (2017).
[29] Y. Yu, D. He, S. Zhang, O. Cojocaru-Mirédin, T. Schwarz, A. Stoffers, X. Wang, S. Zheng, B. Zhu, and C. Scheu, Nano Energy **37**, 203 (2017).
[30] L. Lu, Y. Shen, X. Chen, L. Qian, and K. Lu, Science **304**, 422 (2004).
[31] J. Mao, Y. Wang, Z. Liu, B. Ge, and Z. Ren, Nano Energy **32**, 174 (2016).
[32] A. Stoffers, B. Ziebarth, J. Barthel, O. Cojocaru-Mirédin, C. Elsässer, and D. Raabe, Phys. Rev. Lett. **115**, 235502 (2015).
[33] H. Li, X. X. Liu, Y. S. Lin, B. Yang, and Z. M. Du, Phys. Chem. Chem. Phys. **17**, 11150 (2015).
[34] Y. Zhou, X. Gong, B. Xu, and M. Hu, J. Appl. Phys. **122**, 85105 (2017).
[35] R. W. Cahn, Adv. Phys. **3**, 363 (1954).
[36] A. Foitzik, W. Skrotzki, and P. Haasen, Mater. Sci. Eng., A **132**, 77 (1991).
[37] Y. Zhou, X. Zhang, and M. Hu, Nano Lett. **17**, 1269 (2017).
[38] M. Dixon and M. J. Gillan, Philos. Mag. B **43**, 1099 (1981).
[39] S. Plimpton, J. Comput. Phys. **117**, 1 (1995).
[40] K. A. McCarthy and S. S. Ballard, J. Appl. Phys. **31**, 1410 (1960).
[41] J. P. Perdew, Phys. Rev. B **33**, 8822 (1986).
[42] H. J. Monkhorst and J. D. Pack, Phys. Rev. B **13**, 5188 (1976).
[43] T. C. Harman, P. J. Taylor, M. P. Walsh, and B. E. LaForge, Science **297**, 2229 (2002).
[44] Y. Tian, B. Xu, D. Yu, Y. Ma, Y. Wang, Y. Jiang, W. Hu, C. Tang, Y. Gao, and K. Luo, Nature (London) **493**, 385 (2013).
[45] Q. Huang, D. Yu, B. Xu, W. Hu, Y. Ma, Y. Wang, Z. Zhao, B. Wen, J. He, and Z. Liu, Nature (London) **510**, 250 (2014).
[46] K. Sääskilahti, J. Oksanen, J. Tulkki, and S. Volz, Phys. Rev. B **90**, 134312 (2014).
[47] K. Sääskilahti, J. Oksanen, S. Volz, and J. Tulkki, Phys. Rev. B **91**, 115426 (2015).
[48] R. Rurali, X. Cartoixà, and L. Colombo, Phys. Rev. B **90**, 041408 (2014).
[49] G. Chen, Phys. Rev. B **57**, 14958 (1998).
[50] S. Mei and I. Knezevic, J. Appl. Phys. **118**, 147 (2015).
[51] Y. Zhou, Y. Chen, and M. Hu, Sci. Rep. **6**, 24903 (2016).
[52] Z. Aksamija and I. Knezevic, Phys. Rev. B **82**, 045319 (2010)
[53] S. Kwon, M. C. Wingert, J. Zheng, J. Xiang, and R. Chen, Nanoscale **8**, 13155 (2016).